RESIDUAL STRAIN AND STRENGTH OF CLAY UNDER SEISMIC LOADING

by

Kenji Ishihara, University of Tokyo
Akira Nagao, Japan Highway Public Corporation
Ryoji Mano, Fudo Construction Co.

ABSTRACT

Several series of dynamic triaxial tests were performed on a partially saturated medium-plastic clay by employing four different time histories in the stroke of the axial load. The test results were summarized in a form of shear stress-residual strain relationship in which the peak in dynamic load time history plus the sustained static shear stress is plotted versus the amount of residual component of shear strain. The test results showed that while the effect of the sustained static shear stress is negligibly small, the confining stress exerts a significant influence on the stress-residual strain relationship. The effects of the confining stress were evaluated in terms of the Mohr-Coulomb type failure criterion, and it was discovered that, while the angle of internal friction does not change whether the loading is dynamic or static, the cohesion component in the dynamic loading increases well over the value of cohesion obtained in the static loading test.

INTRODUCTION

A conventional method of approach to evaluate the stability of slopes during earthquakes has been the so-called pseudo-static method in which the effect of an earthquake is taken into account by an equivalent static force determined as the product of a seismic coefficient and the weight of the potential sliding mass. While the capability of this method of analysis has been a focus of skepticism, the controversy does not appear to have been based on the proper choice of key parameters such as the seismic coefficient and strength of slope-forming materials. While the issue of the seismic coefficient has been discussed extensively in recent years (4), the aspect of soil strength to be incorperated into the analysis has been left unheeded and seldom been the subject of careful discussion.

One of the concepts for the proper choice of the seismic coefficient would be to take up a value corresponding to peak ground acceleration expected to occur at a site in question. If such a seismic coefficient is to be used in the pseudo-static method of analysis, the soil strength must be determined under irregular loading conditions simulating the actual loading during an earthquake and the soil strength should be expressed in terms of the maximum shear stress corresponding to the peak in the time history of acceleration. With

such choice of soil strength in perspective, an attempt was made to test undisturbed soil specimens under irregular loading conditions. The details of the results of these tests are described in the following pages.

TEST EQUIPMENT AND MATERIALS

The conventional triaxial shear test apparatus was incorporated into an electro-hydraulic servo loading system by which any form of axial load history could be applied to test specimens. The irregular time histories stored in the tape recorder were retrieved and transmitted to the actuator to produce controlled motions in the triaxial loading piston (1).

Undisturbed samples of volcanic clay were procured from an intact surface exposed on a mountain slope which had suffered a large-scale landslide at the time of the 1978 January 14 Near-Izu earthquake (M=7.0). The slide area is located at Mitaka-iriya village about 4 km inland from the east coast of the Izu Peninsula in Shizuoka prefecture, Japan. Details of the landslide are described in a paper by Ishihara and Nagao (1983). Several cubic blocks of the clay 50 cm in size were excavated at three nearby places, packed in wooden boxes, and transported carefully to the laboratory. While the soil blocks were still fresh without loss of moisture content, they were trimmed into smaller specimens 5 cm in diameter and 10 cm in length. The small specimens were wrapped with pieces of cellophane paper and stored in a humid room until they were tested. The unit weight of the clay was approximately 13.3 kN/m^3. The specific gravity of the clay was 2.70 and the plasticity index was about 30. The water content of the clay varied between 110 and 140 % and the saturation ratio ranged from 85 to 90 %. The cohesion and angle of internal friction of this clay determined from the result of the conventional triaxial test were 48 kN/m^2 and 17°.

DYNAMIC LOADING SCHEME

The entire loading scheme adopted in the present study is illustrated in Fig. 1. A specimen is first consolidated under a confining pressure, σ_0', as in the static test and then subjected to an initial axial stress, σ_s, under drained conditions. A sequence of an irregular axial load is applied to the test specimen with a relatively small amplitude. In the course of this phase of loading, the specimen deforms to a certain magnitude of residual strain, as designated for example by point B' in Fig. 1. The load with the same time history is again applied to the same test specimen with an increased amplitude. The specimen deforms further to a residual strain indicated by point B'' in the schematic diagram of Fig. 1. Similarly, several sequences of the same irregular load are applied to the same specimen with amplitudes being stepwise increased in each sequence. When the points of the peak axial stress and residual strain such as C', C'' and C'''are connected, it becomes possible to obtain a curve such as the dashed curve shown in Fig. 1. This curve may be deemed as representing the stress-residual strain relationship of soils under a given set of initial shear stress and irregular load conditions. In this type of loading scheme, irregular loads with stepwise increasing amplitudes are

applied to a single specimen in sequence. Therefore, it is likely that the response of the specimen to one sequence of irregular loading is affected by other preceding sequences with smaller amplitudes. Inasmuch as the execution of the previous load sequences acts towards increasing strains, their effects on the stress-strain relation may appear as if the specimen were less stiff as compared to a fresh specimen free from any such load history. However, for partially saturated or dry soils, the application of preceding load sequences tend to increase the density, resulting in a certain amount of increase in stiffness. In spite of these load history effects in one way or another, the loading scheme as above may well be considered appropriate to produce a stress-residual strain relation which is representative of that encountered in in-situ soils under seismic loading conditions. It is to be noted that the dynamic test scheme as above has an advantage that a stress-residual strain relation can be obtained using a single test specimen.

In parallel with the dynamic test as above, a series of conventional type static test was conducted under varying confining stresses using the same triaxial test apparatus.

IRREGULAR WAVE FORMS USED IN THE TESTS

The irregular load pattern used in the present tests are four series of time histories of the horizontal accelerations that were obtained on the surface of medium dense sand deposits at Hachinohe and Muroran harbors at the time of the Tokachioki earthquake of 1968. These time histories are shown in Fig. 2. The acceleration time history of the EW-component at Muroran is shown in Fig. 3(a). All these wave forms except the EW of Hachinohe have a few predominant peaks and are classified accordingly as the shock type wave (1). The EW-component at Hachinohe has several large spikes and is classified as the vibration type wave form. Both types of wave forms are assumed as representative of the irregular load pattern to which the ground consisting of relatively stiff materials is subjected during earthquakes.

TEST PERFORMANCE

In the complicated history of stress change, it is always possible to locate a spike where a maximum shear stress occurs. When this stress change is transferred to a specimen by the up-and-down movement of the triaxial loading piston, one of the loading modes is to orient the stress time change so that the peak can be attained when the piston reaches the lowest position. This type of test will be referred to as CM-test (1). It is also possible to have the peak stress oriented so that the peak is executed at the highest position of the loading piston. This type of test will be referred to as EM-test. For each of the wave forms used, both types of test were performed in the present investigation.

One of the results of such series of tests is shown in Fig. 3. The test was of the CM-type and the strength of the specimen from the same sample batch in the static loading test was σ_f = 84.4 kN/m^2, where σ_f denotes the axial stress at failure. The initial axial stress, σ_s, 70 % of the static strength was used in this test. Fig. 3(a) shows the

time history of the EW-component of the acceleration at Muroran which was converted to the axial stress in the triaxial test apparatus. Fig. 3(b) shows the time change of axial strain recorded in one of the test sequences where the amplitude of peak axial stress was σ_d = 87.5 kN/m^2 in the direction of triaxial compression. It is observed that the residual axial strain produced in the specimen by the application of the irregular load was ε_{re} = 2.12 % in this sequence. Before executing this load sequence, the test specimen had already sustained a residual strain of ε'_{re} = 1.88 % in a preceding sequence of the test. Fig. 3(c) shows the time change of the axial strain recorded in the subsequent test sequence in which the amplitude of the irregular load was raised to σ_d = 110.7 kN/m^2. The specimen having sustained a axial strain of ε'_r = 4.0 % in the preceding sequences experienced an addition residual strain of ε_r = 5.85 % in the course of the current loading sequence. In the last sequence, the specimen underwent a residual strain as large as 10.9 % as indicated in Fig. 3(d).

An example of similar test sequences employing a reversely oriented wave form (EM-test) is demonstrated in Fig. 4. The specimen used in this test slowed approximately the same static strength of σ_f = 84.4 kN/m^2. The time changes in the axial strain shown in Figs. 4(b), (c), and (d), are construed in the same way as in the case of the results of the CM-test shown in Fig. 3. It is to be noted that the amplitude of the peak, σ_d, indicated in Fig. 4 refers to the maximum spike on the side of triaxial compression. In the type of triaxial test procedures employed in the present study, the initial shear stress, σ_s, is applied towards the triaxial compression side, and therefore the key phenomena such as residual strains and failure of test specimens are always induced on the side of triaxial compression. Accordingly, it is considered reasonable to take up the peak stress on the triaxial compressioin side as a key variable directly influencing the development of the residual strains and failure of the specimen.

TEST RESULTS

The time histories of the recorded axial strains shown in Figs. 3 and 4 indicate that major part of the residual strains is produced when the peak axial stress is applied to the specimen, and the irregular load after the advent of the peak exerts virtually no influence on the development of additional residual strain. This appears to imply that large displacements or failure produced in clay slopes during earthquakes take place almost at the same time as the peak shear stress is applied to soil elements in the field.

In order to establish the stress-residual strain relationships as illustrated in Fig. 1, values of the total residual strain, $\varepsilon'_{re} + \varepsilon_{re}$, accumulated up to the current sequence of irregular loading tests were read off from the test records such as those shown in Figs. 3 and 4, and these values were plotted versus the peak amplitude of the current irregular loading, σ_d, plus the initial axial stress, σ_s. Note that the peak amplitude, σ_d, plotted, refers to the peak on the triaxial compression side. The results of such data compilation for the cases of the tests shown in Figs. 3 and 4 are presented in Fig. 5. In this plot, the combined static and dynamic axial stress, $\sigma_s + \sigma_d$ is shown normalized to the static strength, σ_f, in order to discern the effect of dynamic loading as against the static behavior. In Fig. 5 the data

points indicated by arrows are those which were read off directly from the test results shown in Figs. 3 and 4. It may be seen in Fig. 5 that there is some difference in the stress-residual strain relationship between the CM- and EM-tests, but overall both test results give a consistent trend. It is of interest to note that the residual strain begins to increase abruptly when the axial stress, $\sigma_d + \sigma_s$, reached a value about 80 % greater than the static strength. Also indicated in Fig. 5 are the stress-strain curves for the static phase of loading until the initial shear stress, σ_s, is increased to 70 % of the static strength. The static stress-strain curves which would have been obtained if the loading had been continued further up are shown in Fig. 5 by dashed lines. It may be seen in Fig. 5 that the stress-strain curve for the static-dynamic loading is located far above the stress-strain curve for the static loading alone. This fact indicates that if the soil specimen is subjected to a dynamic load after it has deformed statically to some extent, the specimen tends to show a larger stiffness and higher strength than it is loaded to failure all the way in static conditions. For a volcanic clay soil as tested in the present study, the increase in strength in the dynamic loading over that in the static loading condition amounts to almost 100 % as indicated in Fig. 5. Such an increase in soil strength appears to emerge from highly rate-dependent nature of cohesive soils when subjected to rapid loads such as those used in the present test scheme. This aspect of the problem is discussed more in detail elsewhere (2).

(1) Effects of Initial Shear Stress

In order to examine the effects of initial shear stress on the stress-residual strain relationship, several series of tests were conducted on the volcanic clay samples by employing the initial static axial stresses varying from σ_s/σ_f = 0.2 to 0.9. In these test series, all the test specimens were consolidated under a confining stress of σ_0' = 50 kN/m , and four different time histories of axial load were used as the irregular load pattern for each test series.

The result of a test series employing an initial shear stress 70 % of the static strength are presented in Figs. 6. Although there exist some scatters depending on the kind of time histories and their orientation (CM or EM), all data points fall in a narrow zone enclosed by dashed lines in Fig. 6. A reasonable average curve is, therefore, drawn through the entire set of data. Fig. 6 shows that the axial stress required to cause failure strain is about 1.95 times as much as the strength under the static loading conditions.

The results of all other test series were similarly represented by average curves and brought together as demonstrated in Fig. 7. The set of summary curves in Fig. 7 shows that the stress-residual strain curve tends to flatten to some extent, as the initial shear stress is increased from 20 % to 90 % of the static strength value. It is somewhat surprising to see that even at a large level of the initial shear stress of σ_s/σ_f = 0.9, the stress-residual strain curve still stays far above the static stress-strain curve. It is likely that with increasing initial shear stress above 90 % of the static strength, the stress-residual strain curve would drop sharply to coincide eventually with the static stress-strain curve. One of the important conclusions drawn from the plot of Fig. 7 is that the stress-residual strain

relationship is not appreciably affected by the initial shear stress, if its value stays within the range of σ_s/σ_f = 0.5 and 0.8, which is generally the case with stress conditions in in-situ deposits of soils under slopes. Consequently, the effect of the initial sustained shear stress on the dynamic stress-strain relation is considered as being of secondary importance, and its effect may be neglected, if a rough estimate is to be made for stability of slopes during earthquakes.

(2) Effects of Confining Stress

For the purpose of examining the effects of confining stress, several series of tests were conducted on the volcanic clay samples by employing three confining pressures of σ_0' = 20, 50 and 80 kN/m^2 . In each series of these tests, specimens were consolidated under a specified confining stress and then subjected to the initial shear stress equal to 70 % of the static strength. The dynamic tests employing the four different time histories were then carried out. The reason why the identical initial shear stress of $\sigma_s = 0.7\sigma_f$ was employed throughout all these test series was that the stress-residual strain relationship is not influenced significantly as corroborated by the afore-mentioned series of tests and that the value of σ_s/σ_f = 0.7 is deemed as corresponding to a representative pre-earthquake state of stress existing in in-situ soils under slopes.

The results of a test series employing a confining stress of 20 kN/m^2 are demonstrated in Fig. 8(a). A reasonable average curve is drawn through the entire set of data both for static and dynamic portions of the stress-residual strain curves. It may be seen that, as soon as the loading is switched into the dynamic phase, the stress-residual deformation curve becomes steeper and eventually converges to a horizontal line corresponding to a dynamic strength value which is about 2.15 times as much as the static strength. The stress-residual strain curve presented in Fig. 6 can also be regarded as a case of the present test series in which the confining stress is σ_0' = 50 kN/m^2. The same characteristic behavior is observed in Fig. 6 as in the case of σ_0' = 20 kN/m^2, but the degree of increase of the dynamic strength over the static strength is seen to be about 1.95 times the static strength, a smaller value as against 2.15 times for the case of the confining stress of 20 kN/m^2. The results of still other test series employing the confining stress of 80 kN/m^2 are presented in Fig. 8(b). The average curve in this figure indicates that the strength in the dynamic loading conditions is approximately 65 % greater than the strength attained under the static conditions. The average stress-residual strain curves demonstrated in Figs. 8(a), 6 and 8(b) are assembled and plotted in Fig. 9 for comparison purposes. Also indicated by dashed lines in Fig. 9 are the stress-strain curves which would have been obtained if the loading had been continued further under static conditions. It can generally be seen that the effect of the dynamic phase of loading is conspicuous and acts towards increasing the stiffness as well as the ultimate strength of the soil.

RELATIONSHIP BETWEEN DYNAMIC AND STATIC STRENGTH

Several series of the tests described in the foregoing sections revealed that the magnitude of static initial shear stress does not

significantly alter the subsequent behavior of the soil subjected to dynamic loads, if the initial shear stress lies within the range of 40 to 90 % of the strength value obtained in the static loading conditions. Therefore, the influence of the initial shear stress will be neglected in the following analysis.

It was discovered in the tests that the effect of the confining stress is appreciable and can not be neglected in evaluating the residual strains and strength in the dynamic loading conditions. This consequence may be taken for granted because the strength of partially saturated cohesive soils in static conditions has been known generally to vary with the magnitude of the confining stress. The effect of the confining stress on the static strength of soils has been evaluated in terms of the apparent angle of internal friction defined as an angle of slope in the Mohr circle representation of failure state in the stress space. Therefore, it is of interest to establish a Mohr-Coulomb type failure criterion for the dynamic loading condition as well and compare it with the convential failure criterion for the static loading condition. The method adopted in the present study for establishing the dynamic failure criterion is illustrated in Fig. 10. The value of the confining stress, σ_0', is first laid off at point A in abscissa and then the static and dynamic strength values are laid off towards the right as AB and AC, respectively. The circle drawn through points A and B is the Mohr circle associated with falilure in the static loading. Likewise, the Mohr circle for failure in the dynamic loading can be constructed by drawing a circle through points A and C, as shown in Fig. 10.

Using the above procedures, two sets of Mohr circles specifying failure in static and dynamic loading conditions were established for the test data on the volcanic clay presented in Fig. 8. The Mohr circles thus constructed are shown in Fig. 11. It is also possible to draw a straight envelop line for each set of the Mohr circles shown in Fig. 11. For the volcanic clay from Izu region, the cohesion component for static loading, C, was 20 kN/m^2 and the cohesion for dynamic loading, C , was 48 kN/m^2. It is of particular interest to note that the angle of internal friction was practically the same both for the static and dynamic loading conditions. The angle of internal friction, ϕ, for the clay tested was 17°. The fact that the effect of dynamic loading on the failure strength is manifested only through the cohesion component may be taken as reasonable if one is reminded of the fact that the increase in strength due to rapid loading such as the seismic irregular loading emerges mainly from the viscous nature of soil materials. This aspect of soil properties is discussed in some detail elsewhere (2).

On the basis of the conclusion that the angle of internal friction is identical both in the static and dynamic loading conditions, it becomes possible to deduce some correlation between the strength parameters pertaining to these two loading conditions. Suppose the angle of internal friction, ϕ, and cohesion, C, in the static loading are known for a given soil, then the axial stress required to cause failure, σ_f, under a confining stress, σ_0', is given by,

$$\sigma_f = \frac{2\sin\phi}{1-\sin\phi}\,\sigma_0' + \frac{2C\cos\phi}{1-\sin\phi} \qquad \cdots\cdots(1)$$

This is the well known equation expressing the straight-line failure envelop in Fig. 10. When a dynamic test is performed under the same confining stress, the axial stress causing failure, σ_{Df}, is given by,

$$\sigma_{fD} = \frac{2\sin\phi}{1-\sin\phi}\,\sigma_0' + \frac{2C_D\cos\phi}{1-\sin\phi} \qquad \cdots\cdots(2)$$

Combining Eqs. (1) and (2), one obtains,

$$\frac{C_D}{C} - 1 = \left(1 + \frac{\sigma_0'}{C\cot\phi}\right)\left(\frac{\sigma_{Df}}{\sigma_f} - 1\right) \qquad \cdots\cdots(3)$$

Thus, knowing the static strength parameters, C and ϕ, one can estimate the dynamic cohesion value, C_D, from Eq. (3), if a single dynamic test is run to determine the value of the dynamic strength, σ_{Df}, under an appropriate confining stress, σ_0'. Once the value of the dynamic cohesion is thus known, it becomes in turn possible to estimate the dynamic strength, σ_{Df}, for any other value of the confining stress through the use of Eq. (2).

CONCLUSIONS

Several series of dynamic triaxial shear tests were conducted on a partially saturated volcanic clay with a medium plasticity index by employing four different time histories in the stroke of the axial load. The test results showed that the effects of sustained static shear stress on the residual strain and failure can be neglected, if the static shear stress stays within 40 to 90 % of the strength determined under the conventional static loading conditions. It was shown, however, that the effects of confining stress are significant and can be evaluated in terms of the Mohr-Coulomb type failure criterion. In fact, scrutiny of the test data disclosed that, while the cohesion component in the dynamic loading is increased over that in the static loading, the angle of internal friction remains practically unchanged whether the loading is dynamic or static. For the clay tested, the cohesion component in the dynamic loading was shown to increase to 2.4 times the value of cohesion obtained in the static loading. On the basis of the assumption that the angle of internal friction is not influenced by the mode of loading, a relationship was established between static and dynamic strength enabling the latter to be assessed from the strength parameters associated with the static loading.

ACKNOWLEDGEMENTS

Dynamic triaxial shear tests in the laboratory were performed with the assistance of Messrs. M. Higashi and s. Kurashima, Appreciation is expressed for the cooperation of these persons.

REFERENCES

(1) Ishihara, K. and Yasuda, S. (1973), "Sand Liquefacion under Random Earthquake Loading Conditions," Proc. 5th World Conference on Earthquake Engineering, Session ID, 38.

(2) Ishihara, K. (1981), "Strength of Cohesive Soils under Transient and Cyclic Loading Conditions," State-of-the-Art in Earthquake Engineering, edited by Ergunay and Erdik, Turkish National Committee on Earthquake Engineering, pp.154-169.

(3) Ishihara, K. and Nagao, A. (1983), "Analysis of Landslides during the 1978 Izu-Ohshima-Kinkai Earthquake," Soils and Foundations, Vol.23, No.1, pp.141-159.

(4) Seed H.B. and Martin G.R. (1966), "The Seismic Coefficient in Earth Dam Design," Proc. ASCE. Vo.92, SM3, pp.25-60.

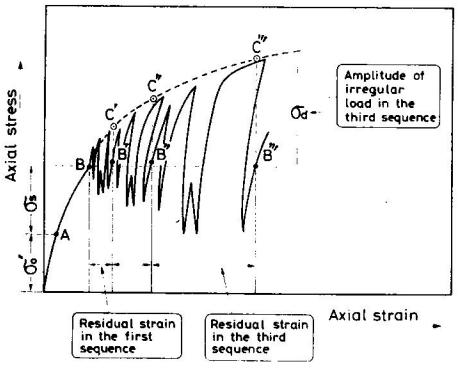

Fig. 1 Loading scheme used in the tests

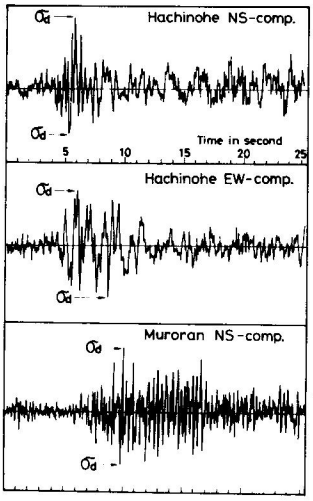

Fig. 2 Irregular time histories of loads used in the tests

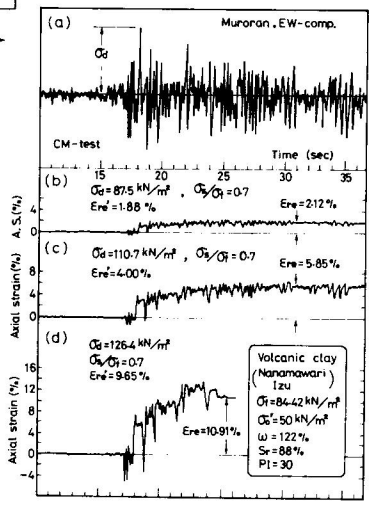

Fig. 3 Evolvement of residual strains in the irregular loading test

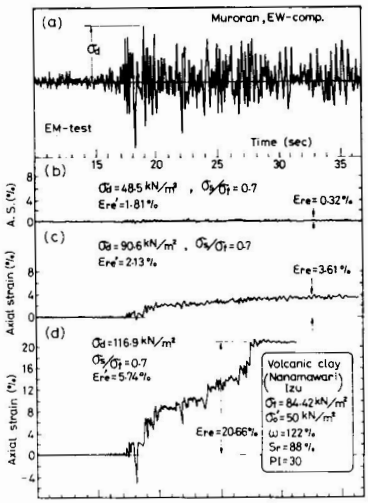

Fig. 4 Evolvement of residual strains in the irregular loading test

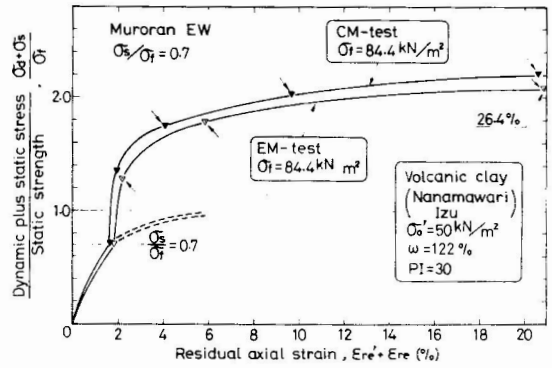

Fig. 5
Shear stress-residual strain relationship

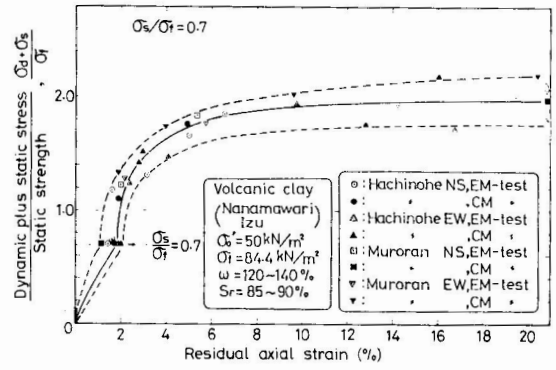

Fig. 6
Shear stress-residual strain relationships for different irregular loads

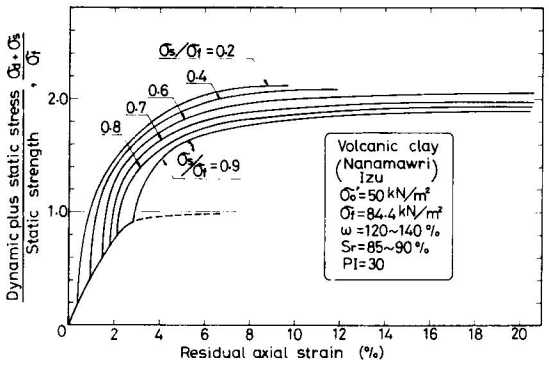

Fig. 7
Summary of Stress-residual strain relationships for different initial shear stresses

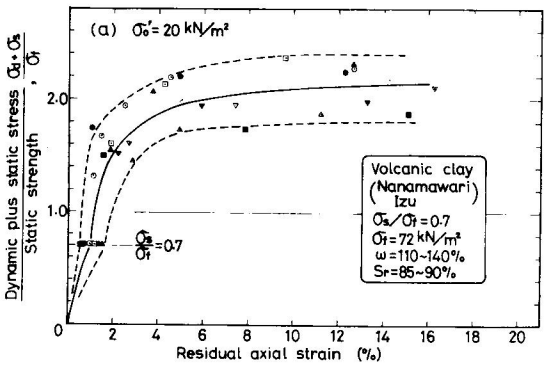

Fig. 8(a)
Shear stress-residual strain relationships for different confining stresses

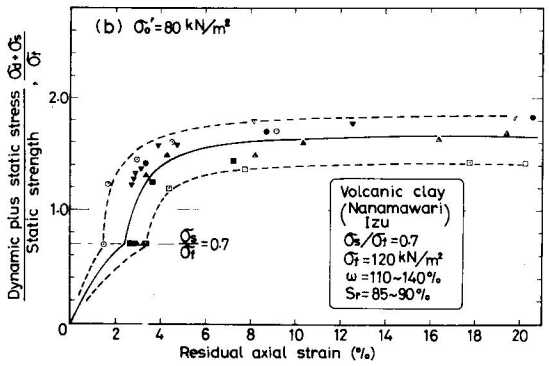

Fig. 8(b)

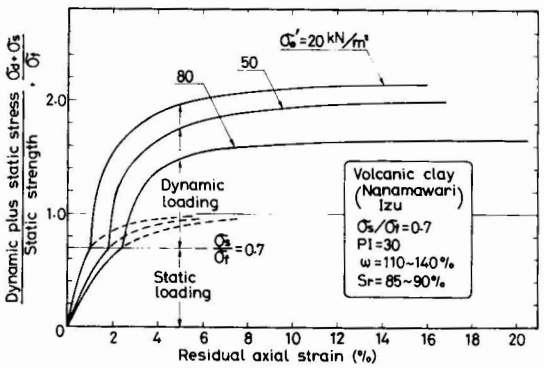

Fig. 9
Summary of stress-residual strain relationships for different confining stresses

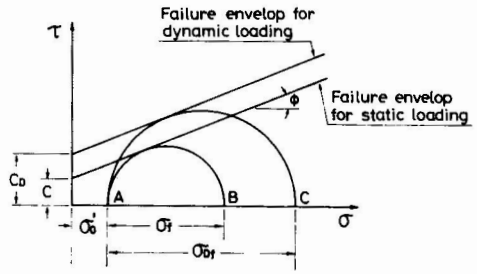

Fig. 10
Construction of Mohr circles and failure envelops associated with static and dynamic loading

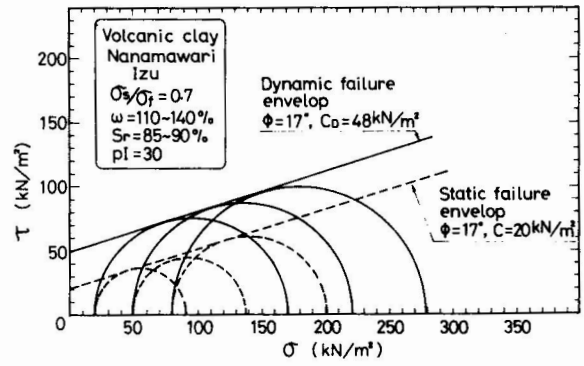

Fig. 11
Failure envelops obtained from static and dynamic loading test results